Molecular Neurobiology (2019) 56:1196–1210
https://doi.org/10.1007/s12035-018-1140-7

# Cocaine Blocks Effects of Hunger Hormone, Ghrelin, Via Interaction with Neuronal Sigma-1 Receptors

David Aguinaga[1,2] · Mireia Medrano[1,2] · Arnau Cordomí[3] · Mireia Jiménez-Rosés[3] · Edgar Angelats[1,2] · Mireia Casanovas[1,2] · Ignacio Vega-Quiroga[4] · Enric I. Canela[1,2] · Milos Petrovic[5] · Katia Gysling[4] · Leonardo Pardo[3] · Rafael Franco[1,2,7] · Gemma Navarro[1,6,7]

Received: 1 December 2017 / Accepted: 21 May 2018 / Published online: 7 June 2018


## Abstract

Despite ancient knowledge on cocaine appetite-suppressant action, the molecular basis of such fact remains unknown. Addiction/eating disorders (e.g., binge eating, anorexia, bulimia) share a central control involving reward circuits. However, we here show that the sigma-1 receptor ($\sigma_1$R) mediates cocaine anorectic effects by interacting in neurons with growth/hormone/secretagogue (ghrelin) receptors. Cocaine increases colocalization of $\sigma_1$R and GHS-R1a at the cell surface. Moreover, in transfected HEK-293T and neuroblastoma SH-SY5Y cells, and in primary neuronal cultures, pretreatment with cocaine or a $\sigma_1$R agonist inhibited ghrelin-mediated signaling, in a similar manner as the GHS-R1a antagonist YIL-781. Results were similar in G protein-dependent (cAMP accumulation and calcium release) and in partly dependent or independent (ERK1/2 phosphorylation and label-free) assays. We provide solid evidence for direct interaction between receptors and the functional consequences, as well as a reliable structural model of the macromolecular $\sigma_1$R-GHS-R1a complex, which arises as a key piece in the puzzle of the events linking cocaine consumption and appetitive/consummatory behaviors.

**Keywords** Neuroendocrine · Drug addiction · Receptor heteromer · G protein-coupled heteroreceptor complex · Functional selectivity · Cross-regulation

## Introduction

Used today as a recreational drug, cocaine was first consumed by humans in the form of coca leaves. Indigenous peoples of South America, especially those living at higher altitude, were aware that chewing coca leaves helped to keep their life style. For example, *Erythroxylum coca* was used to facilitate traversing long distances across the Andes with reduced weight and

Rafael Franco and Gemma Navarro contributed equally to this work.

**Electronic supplementary material** The online version of this article (https://doi.org/10.1007/s12035-018-1140-7) contains supplementary material, which is available to authorized users.

✉ Rafael Franco
rfranco123@gmail.com; rfranco@ub.edu

✉ Gemma Navarro
dimartts@hotmail.com

[1] Centro de Investigación en Red, Enfermedades Neurodegenerativas (CIBERNED), Instituto de Salud Carlos III, Madrid, Spain

[2] Department of Biochemistry and Molecular Biomedicine, School of Biology, Universitat de Barcelona, Barcelona, Spain

[3] Laboratori de Medicina Computacional, Unitat de Bioestadística, Facultat de Medicina, Universitat Autònoma de Barcelona, 08193 Bellaterra, Spain

[4] Department of Cellular and Molecular Biology, Faculty of Biological Sciences, Pontificia Universidad Católica de Chile, Santiago, Chile

[5] School of Pharmacy and Biomedical Sciences, University of Central Lancashire, Preston PR1 2HE, UK

[6] Department of Biochemistry and Physiology, Faculty of Pharmacy, Universitat de Barcelona, Barcelona, Spain

[7] School of Biology, Universitat de Barcelona, Diagonal 643, 08028 Barcelona, Spain

little food. Despite such ancient knowledge, i.e., the appetite suppressant action of cocaine, the molecular basis of hunger prevention remains unknown. This report was undertaken to test the hypothesis of whether the well-known anorexigenic effect of cocaine is mediated by growth hormone secretagogue (GHS) receptors, also known as ghrelin receptors, which are key players in the central control of food/energy intake [1].

Ghrelin, the "hunger" endocrine hormone, is involved in the control of food intake and energy homeostasis [2]. Its action is mediated by, up-to-date, only one specific ghrelin receptor that belongs to the superfamily of G protein-coupled receptors (GPCRs). In humans, alternative splicing leads to: isoform 1a that contains seven transmembrane (TM) helices (GHS-R1a, 366 amino acids) and isoform 1b that lacks 6 and 7 TM helices (GHS-R1b, 289 amino acids) [3–5]. These TM domains are required for ligand binding and coupling to heterotrimeric G proteins and, therefore, ghrelin cannot signal via the GHS-R1b isoform [6]. GHS-R1b seems to serve as a modulator of GHS-R1a surface expression and signaling [7]. In fact, GHS-R1b is expressed in the same cells as GHS-R1a, and both isoforms interact to form heteromer receptor signaling units [6]. We have previously shown that GHS-R1b guides surface expression of functional GHS-R1a, acting as a dual modulator: low relative GHS-R1b expression potentiates GHS-R1a function, while high relative GHS-R1b expression inhibits GHS-R1a function [7]. GHS-R1b negatively influences ghrelin action by allosteric interactions within the GHS-R1a-GHS-R1b heteromer that reduce the efficacy of the hormone [6, 8]. Although the purified GHS-R1a, assembled into lipid discs is reportedly coupled to $G_{q/11}$ [9], the receptor may also couple to non-$G_{q/11}$ heterotrimeric G proteins (www.guidetopharmacology.org). Indeed, we previously found preferential $G_{i/o}$ coupling of the GHS-R1a-GHS-R1b complex in HEK-293T cells and preferential $G_{s/olf}$ coupling in both striatal and hippocampal neurons in culture [7]. Heteromerization of GHS-R1a and GHS-R1b in heterologous expression systems is often needed for proper ghrelin-induced signaling. It should be noted that ghrelin receptors may form direct protein-protein interactions with a variety of GPCRs, inter alia with dopamine, melanocortin, prostanoid, serotonin, somatostatin, neurotensin, and GPR83 receptors [10]; see www.gpcr-hetnet.com and references therein.

The sigma-1 receptor ($\sigma_1$R) is an atypical membrane protein, whose exact function remains unknown. It has been proposed that it functions as a pluripotent cell function modulator in living cells [11] and is attracting a lot of interest due to its potential as a target against neuropathic pain [12–14]. While its physiological function remains elusive and the endogenous ligand is yet to be discovered, $\sigma_1$R is a protein target for cocaine [15–17]. Drugs blocking the interaction of cocaine with $\sigma_1$R have been proposed to reduce drug-seeking behavior [18]. $\sigma_1$R-mediated cocaine actions in the central nervous system are dependent on its interactions with GPCRs. For instance, we have identified that cocaine binding to $\sigma_1$R potentiates dopamine $D_1$R-mediated adenylate cyclase signaling [19, 20] and inhibits $D_2$R-mediated signaling in striatal neurons [20]. These actions disrupt the delicate balance between inputs of reward seeking controlled by $D_1$R-containing neurons and inputs of aversion coming from $D_2$R-containing neurons. In addition, cocaine binding to $\sigma_1$R also induces disruption of the orexin and corticotropin-releasing factor receptor negative cross-talk, playing an important role in the stress-induced cocaine-seeking behavior [21].

We show in this manuscript that $\sigma_1$R interacts with and modulates the activity of GHS-R1a, indicating a non-previously suspected receptor interplay. Moreover, because structural information on GPCR homomeric complexes already exist [22] and the crystal structure of $\sigma_1$R has been recently elucidated [23], we have devised a molecular arrangement consisting of the GHS-R1a-GHS-R1b heteromer in complex with $\sigma_1$R. We have taken advantage of the recent knowledge showing that $\sigma_1$R arranges as a homotrimer (each protomer with a single TM). We used synthetic peptides with the amino acid sequences from the TM helices of GHS-R1a, together with bimolecular fluorescence complementation assays and computer modeling, to find the oligomerization interfaces between GHS-R1a, GHS-R1b, and $\sigma_1$R, and to propose a structural model of the macromolecular complex.

## Materials and Methods

### Reagents

Cocaine-chlorhydrate was provided by the Spanish *Agencia del Medicamento* (ref no.: 2003C00220). $\sigma_1$R (PRE-084), GHs-R1a (ghrelin and YIL-781), and $A_1$ adenosine receptor (L-phenylisopropyl adenosine, R-PIA, and 1,3-dipropyl-8-cyclopentylxanthine, DPCPX) ligands were purchased from Tocris, Bristol, UK. Cocaine-chlorhydrate used for the acute and chronic administration was donated by the National Institute of Drug Abuse, USA, to K. Gysling, Chile.

### Fusion Proteins and Expression Vectors

Sequences encoding amino acid residues 1–155 and 155–238 of the Venus variant of yellow fluorescence protein (Venus) were subcloned in the pcDNA3.1 vector to obtain complementary Venus N- and C-hemiproteins. Human cDNAs for GHS-R1a, GHS-R1b, or $\sigma_1$R were amplified without their stop codons using sense and antisense primers harboring: EcoRI and KpnI sites to be subcloned in pcDNA3.1RLuc vector (p*RLuc*-N1 PerkinElmer, Wellesley, MA) or in a $GFP^2$-containing vector (p-$GFP^2$, Packard BioScience, Meridien, CT) to provide $\sigma_1$R-Rluc, GHS-R1a-Rluc, GHS-R1a-YFP, $\sigma_1$R-YFP, or GHS-R1a-$GFP^2$ plasmids. Human

cDNA for $A_{2A}R$ was subcloned into p-$GFP^2$ vector harboring HindIII and BamHI sites to provide the encoding $A_{2A}$-$GFP^2$ plasmid. For bimolecular fluorescence complementation (BiFC) experiments, cDNA for GHS-R1b, GHS-R1a, and $\sigma_1R$ were subcloned into pcDNA3.1-nVenus and pcDNA3.1-cVenus harboring EcoRI and KpnI sites to provide plasmids encoding GHS-R1b-nYFP, GHS-R1b-cYFP, GHS-R1a-nYFP, and $\sigma_1R$-cYFP.

## Cell Lines, Neuronal Primary Cultures, and Transient Transfection

HEK-293T human embryonic kidney cells were grown in Dulbecco's modified Eagle's medium (DMEM) (Gibco) supplemented with 2 mM L-glutamine, 100 μg/ml sodium pyruvate, 100 U/ml penicillin/streptomycin, MEM Non-Essential Amino Acid Solution (1/100) and 5% (*v*/*v*) heat-inactivated fetal bovine serum (FBS) (all supplements were from Invitrogen, Paisley, Scotland, UK). Primary cultures of striatal neurons were obtained from fetal Sprague Dawley rats of 19 days. Cells were isolated as described in Hradsky et al. [24] and plated at a confluence of 40,000 cells/0.32 $cm^2$. Cells were maintained for 12 days in Neurobasal medium supplemented with 2 mM L-glutamine, 100 U/ml penicillin/streptomycin, and 2% (*v*/*v*) B27 supplement (GIBCO) in 6-well microplates. Cells were transiently transfected with the corresponding cDNAs using the PEI (PolyEthylenImine, Sigma-Aldrich, St. Louis, MO, USA) method or, in the case of the anti-$\sigma_1R$ siRNA, with Lipofectamine 2000 (Thermo Fisher Scientific). After transfection, cells were incubated in serum-free medium which was replaced by complete medium after 4 h. Experiments were carried out 48 h later (unless otherwise indicated).

## Immunocytochemistry

HEK-293T cells were fixed in 4% paraformaldehyde for 15 min and washed with PBS containing 20 mM glycine to quench free aldehyde groups. After permeabilization with PBS-glycine buffer containing 0.2% Triton X-100 for 5 min, cells were blocked with PBS containing 1% bovine serum albumin (1 h at room temperature). $\sigma_1R$-YFP was detected by its own fluorescence (wavelength 530 nm), and Rluc-containing proteins were stained using a mouse monoclonal anti-Rluc antibody (1/200, 1 h, room temperature, Millipore, CA, USA) and a Cyn3-conjugated donkey anti-mouse antibody (1/200, Jackson Immunoresearch Laboratories, West Grove, PA, USA). Nuclei were stained with Hoechst (1/100, Sigma-Aldrich, St. Louis, USA) and samples were mounted with Mowiol 30% (Calbiochem) and observed in a Leica SP2 confocal microscope (Leica Microsystems, Mannheim, Germany).

## Resonance Energy Transfer

For bioluminescence energy transfer (BRET) assays, HEK-293T cells were transiently transfected with a constant amount of cDNA for $\sigma_1R$-Rluc and increasing amounts of cDNAs for GHS-R1a-$GFP^2$ or $A_{2A}$-$GFP^2$. To normalize the number of cells, protein concentration was determined using a Bradford assay kit (Bio-Rad, Munich, Germany) using bovine serum albumin dilutions as standards. To quantify fluorescence, cell suspensions were distributed in 96-well microplates (black with transparent bottom), and fluorescence was read in a Fluostar Optima Fluorimeter (BMG Labtech, Offenburg, Germany) equipped with a high-energy xenon flash lamp, using a 10 nm bandwidth excitation filter (400 nm). For BRET measurements, cell suspensions (20 μg protein) were distributed in 96-well white microplates (Corning 3600, Corning, NY), and 5 μM DeepBlueC (Molecular Probes, Eugene, OR) was added right before BRET signal acquisition using a Mithras LB 940 reader (Berthold Technologies, DLReady, Germany). To quantify receptor-Rluc expression, luminescence readings were performed after 10 min of adding 5 μM coelenterazine H. Net BRET is defined as [(long-wavelength emission)/(short-wavelength emission)] − $C_f$, where $C_f$ corresponds to [(long-wavelength emission)/(short-wavelength emission)] for the Rluc protein when expressed individually. For bimolecular complementation (BiFC) assays, HEK-293T cells were transiently transfected with a constant amount of cDNA encoding for proteins fused to nVenus or cVenus and incubated for 4 h in complete DMEM containing the interfering TAT peptides (with similar sequences to those in TM1 to TM7 of GHS-R1a; see supplementary Table 1 for sequences). YFP resulting from complementation was detected by placing cells (20 μg protein) in 96-well microplates (black plates with a transparent bottom) and reading the fluorescence in a Fluostar Optima Fluorimeter (BMG Labtech, Offenburg, Germany) using a 30-nm bandwidth excitation filter (485 nm).

## Cytosolic cAMP Determination

Forskolin dose-response curves in different density of cells were performed to select the most appropriate conditions of the assay, which resulted in 5000 HEK-293T cells, 7500 neurons, and 0.5 μM forskolin. Subsequently, assays were performed in medium containing 50 μM zardaverine, placing cells in 384-well microplates. This was done by the preincubation with reagents (the $\sigma_1R$ agonist, PRE-084, the GHS-R1a antagonist, YIL-781, or cocaine) for 15 min, followed by ghrelin addition (100-nM final concentration), and after 15 min incubation period, 50 μM forskolin was added. Readings were performed 15 min later using a homogeneous time-resolved fluorescence energy transfer (HTRF) method requiring the Lance Ultra cAMP kit (PerkinElmer)

and fluorescence readings (at 665 nm) in a PHERAstar Flagship microplate reader equipped with an HTRF optical module (BMG Labtech).

## MAPK Activation

To determine ERK1/2 phosphorylation, 40,000 HEK-293 cells/well or 50,000 neurons/well were plated in transparent Deltalab 96-well microplates and kept in the incubator for 48 h. The medium was substituted by serum-free DMEM medium 2 to 4 h before starting the experiment. Before the addition of 100 nM, ghrelin cells were pretreated (10 min at 25 °C) in serum-free medium with different reagents (the $\sigma_1$R agonist, PRE-084, the GHS-R1a antagonist, YIL-781, or cocaine). After 7 min of ghrelin-induced activation, cells were washed twice with cold PBS before the addition of 30 μL of lysis buffer (20 min). Supernatants (10 μL) were placed in white ProxiPlate 384-well microplates, and ERK1/2 phosphorylation was determined using the AlphaScreen®SureFire® kit (Perkin Elmer) and the EnSpire® Multimode Plate Reader (PerkinElmer, Waltham, MA, USA).

## Intracellular Calcium Mobilization

HEK-293T cells were co-transfected with cDNA(s) for receptor(s) and 1 μg cDNA for the calmodulin-based calcium sensor, GCaMP6 [25]. Forty-eight hours after transfection, cells were detached using $Mg^{2+}$-free Locke's buffer pH 7.4 (154 mM NaCl, 5.6 mM KCl, 3.6 mM $NaHCO_3$, 2.3 mM $CaCl_2$, 5.6 mM glucose, and 5 mM HEPES) supplemented with 10 μM glycine. One hundred fifty thousand cells per well were plated in 96-well black, clear bottom, microtiter plates. Then, cells were incubated with the $\sigma_1$R agonist, PRE-084, the GHS-R1a antagonist, YIL-781, or cocaine for 10 min before ghrelin 100-nM addition. Upon excitation at 488 nm, real-time 515-nm fluorescence emission due to calcium-ion-complexed GCaMP6 was recorded on the EnSpire® Multimode Plate Reader (every 5 s, 100 flashes per well).

## Label-Free Dynamic Mass Redistribution Assays

HEK-293T cells and neuronal primary cultures were seeded in 384-well sensor microplates to obtain 70–80% confluent monolayers constituted by 10,000 HEK-293T cells or 14,000 neurons per well. Before the assay, cells were washed twice with assay buffer (HBSS with 20 mM HEPES and 0.1% DMSO, pH 7.15) and incubated for 2 h in 40 μL/well of assay-buffer in the reader at 24 °C. Hereafter, the sensor plate was scanned, and a baseline optical signature was recorded before adding 10 μL of cocaine (30 μM), PRE-084 (100 nM), or YIL-781 (2 μM) for 30 min followed by ghrelin addition. All compounds were dissolved in assay buffer. Then, dynamic mass redistribution (DMR) responses were monitored for at least 3600 s using an EnSpire® Multimode Plate Reader (PerkinElmer, Waltham, MA, USA). Sensitive measurements of changes in local optical density mimicking cellular mass movements induced upon receptor activation were detected using EnSpire Workstation Software v 4.10.

## Proximity Ligation Assay

For proximity ligation assays (PLAs), primary cultures of striatal neurons were fixed in 4% paraformaldehyde for 30 min and permeabilized in PBS containing 0.05% Triton X-100 (15 min). After 1 h incubation at 37 °C with the blocking solution, primary cultures were incubated overnight with anti-$\sigma_1$R (1/100, Santa Cruz Biotechnology, Dallas, USA), and anti-GHS-R1a antibody (1/100, AbCam, Cambridge, UK) in the presence of Hoechst (1/100, Sigma-Aldrich, St. Louis, USA) to stain nuclei. Cells were processed using the PLA probes that bind to the primary antibodies (Duolink II PLA probe anti-Mouse plus and Duolink II PLA probe anti-Goat minus) and heteroreceptor complex formation was detected using the Duolink II in situ PLA detection Kit (OLink; Bioscience, Uppsala, Sweden). Images were taken in a Leica SP2 confocal microscope (Leica Microsystems, Mannheim, Germany). For each field of view, a stack of two channels (one per staining), and four to six *Z* stacks with a step size of 1 μm were acquired. Quantification of the number of cells containing one or more red dots versus total cells (blue nuclei) and of the number of red dots/cell-containing dots:r ratio was conducted using a dedicated software known as Duolink ImageTool (ref: DUO90806, Sigma-Olink). This software has been developed for PLA signals and cell nuclei quantification in images generated from fluorescence microscopy.

## Cocaine Treatment and Fixation Procedure

Male Sprague-Dawley rats weighing 200–220 g were selected for the experiments. Rats were kept in controlled environment with 12-h light-dark cycle at 21 °C room temperature. Food and water were provided ad libitum. All experimental procedures were approved by the Ethics Committee of the Faculty of Biological Sciences of "Pontificia Universidad Católica de Chile" and followed the international guidelines (NIH Guide for the Care and Use of Laboratory Animals). Rats were divided in two groups of experimental series, chronic cocaine-treated rats with respective control (saline) and acute cocaine rats. The chronic cocaine-administration protocol consisted of 15 mg/Kg, i.p. cocaine injections twice per day for 14 days as described by [26], whereas the acute cocaine treatment protocol consisted of two injections of 15 mg/kg, i.p. cocaine, one in the morning and one in the afternoon. Daily administration of cocaine and saline solution was performed in both

experimental series at the same time in the morning and afternoon (beginning at 11:00 A.M. and 5:00 P.M.). The day after last cocaine injection, rats were deeply anesthetized with ketamine-xylazine (50–5 mg/kg, respectively) and intracardially perfused with 50 ml of saline, followed by 500 ml of 4% paraformaldehyde (PFA) in phosphate buffer. Then, the animals were guillotined, and the brain was post-fixed with 4% PFA for 2 h and left in 20% sucrose during 2 days.

### Computational Model of the GHS-R1a-$\sigma_1$R Heteromer

The structure of $\sigma_1$R was modeled based on the recently released crystal structure (PDB id 5HK1) [27]. The inactive conformation of human GHS-R1a (UniProt: Q92847) was built using crystal structures of the neurotensin 1 receptor (PDB id 4XES for all parts of the receptor, and PDB id 3ZEV for the C-terminal part of TM7 and helix 8) [28, 29]. The human neurotensin 1 receptor and GHS-R1a share 33% of sequence identity and 51% of sequence similarity. The "active-like" form of GHS-R1a was modeled by incorporating the active features present in the crystal structure of the $\beta_2$-adrenergic receptor in complex with $G_s$ (PDB id 3SN6), namely the internal halves of TMs 5 and 6 [30]. The "active-like" model of GHS-R1a contains $G_i$ (PDB id 1AGR) [31]. The GHS-R1a homodimer was constructed based on the symmetric TM5/6 protein-protein interface observed in the crystal structure of the μOR (PDB id 4DKL) [32]. The GHS-R1a-$\sigma_1$R complex was constructed using protein-protein docking with HADDOCK [33], under the imposed experimental restrains that TMs 1 and 2 of GHS-R1a contact the single TM of $\sigma_1$R.

## Results

### GHS-R1a Forms Heteromeric Complexes with $\sigma_1$R

Immunocytochemical assays were performed to detect whether colocalization between GHS-R1a and $\sigma_1$R occurred in transfected HEK-293T cells. Cells were transfected with cDNAs for $\sigma_1$R fused to YFP (0.75 μg cDNA) and for GHS-R1a fused to Renilla luciferase (Rluc) (1.66 μg cDNA). In cells expressing only $\sigma_1$R-YFP, the receptor was detected by YFP fluorescence, identifying $\sigma_1$R-YFP mainly in intracellular structures. In HEK-293T cells expressing GHS-R1a-Rluc, the GHS-R1a was detected by a specific primary anti-Rluc and secondary Cy3 antibodies, the receptor was detected in intracellular structures and at the plasma membrane level. Interestingly, in HEK-293T cells co-expressing $\sigma_1$R-YFP (0.75 μg cDNA) and GHS-R1a-Rluc (1.66 μg cDNA), colocalization of both receptors was observed (Fig. 1a).

To identify a potential direct interaction between $\sigma_1$R and GHS-R1a, we developed BRET experiments, transfecting a constant amount of cDNA for $\sigma_1$R-Rluc (0.075 μg cDNA) and increasing amounts of cDNA for GHS-R1a-GFP$^2$ (0.5 to 3 μg cDNA). A saturation BRET curve was obtained, thus indicating a specific interaction between $\sigma_1$R and GHS-1a ($BRET_{max}$ 371 ± 38 mBU, $BRET_{50}$ 68 ± 23) (Fig. 1b, c). In contrast, when adenosine $A_{2A}$R-GFP$^2$ (0.5 to 2.5 μg cDNA) was used as negative control instead of GHS-R1a receptor, a linear plot with low BRET values was obtained.

### Quaternary Structure of the Heteromeric Complex Between $\sigma_1$R and GHS-R1a

We next addressed the quaternary structure of $\sigma_1$R-GHS-R1a complexes taking advantage of the recent publication of the crystal structure of $\sigma_1$R in a trimeric arrangement. The macromolecular complex cannot be understood without taking into account that the GHS-R1a receptor can form homomeric interactions with GHS-R1a and/or heteromeric interactions with GHS-R1b [6–8]. Thus, to identify the TM interfaces involved in GHS-R1a-GHS-R1a homodimerization, GHS-R1a-GHS-R1b heterodimerization and their TM-interacting interfaces with $\sigma_1$R, we used synthetic peptides with the amino acid sequence of individual 1-7 TM helices of GHS-R1a fused to the transactivator of transcription (TAT) peptide (exact sequences are provided in supplementary Table 1). These cell-penetrating peptides interact with the TM domain of membrane proteins and can selectively disrupt interactions between proteins, i.e., GPCR protomers [34, 35]. These peptides were first tested in HEK-293T cells expressing GHS-R1a-nYFP (0.75 μg cDNA) and GHS-R1a-cYFP (0.5 μg cDNA) to explore whether bimolecular fluorescence complementation (BiFC) occurs (approximately 4,000 units of fluorescence indicative of the formation of GHS-R1a-homodimer complexes). Notably, in the presence of interference peptides, we observed that the fluorescence decreased by twofold only with TM5 and TM6 peptides (Fig. 2a). These results pointed to the TM 5/6 interface for GHS-R1a-GHS-R1a homodimerization. Similar results were obtained for GHS-R1a-GHS-R1b heterodimerization (TM 5/6 interface, Fig. 2b), despite the fact that GHS-R1b isoform lacks TMs 6 and 7. Interestingly, when cells were transfected with cDNAs for GHS-R1a-nYFP, GHS-R1b-cYFP, and non-fused GHS-R1a, fluorescence was reduced in the presence of TM4, TM5, and TM6 peptides (Fig. 2c). These results suggest an arrangement of protomers in which homodimerization of GHS-R1a occurs via the TM 5/6 interface, whereas heterodimerization of GHS-R1a and GHS-R1b occurs via the TM 4/5 interface (Fig. 2d). The fluorescence decrease induced by the TM6 peptide of GHS-R1a (in addition to TM4 and TM5, Fig. 2c) could indicate that this peptide also restricts the interactions with the TM 4 of GHS-R1b (Fig. 2d).

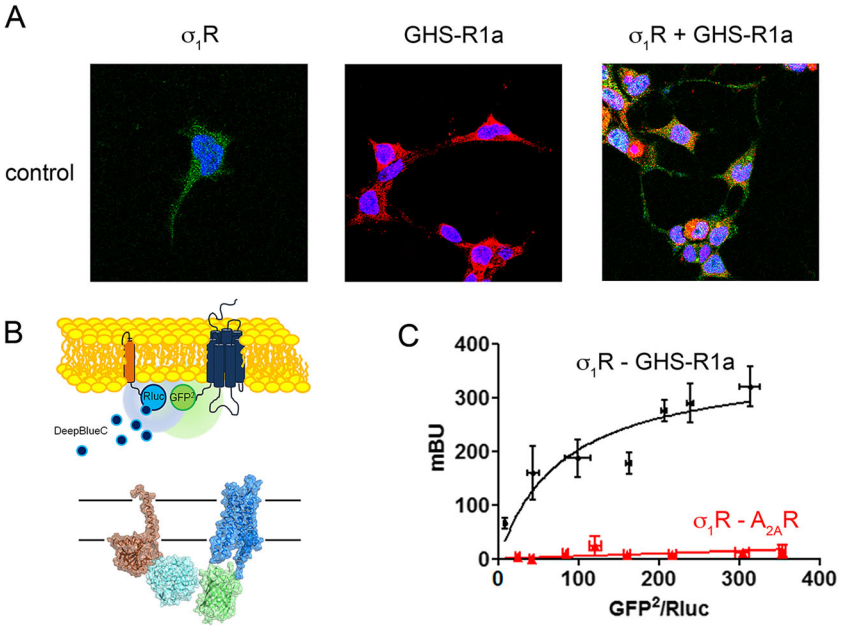


**Fig. 1** GHS-R1a interacts with $\sigma_1$R to form $\sigma_1$R-GHS-R1a heteroreceptor complexes. **a** HEK-293T cells expressing $\sigma_1$R-YFP, GHS-R1a-Rluc, or both were monitored by the YFP fluorescence (green) or using a monoclonal anti-Rluc primary antibody and a cyanine-3-conjugated secondary antibody (red). Colocalization is shown in yellow. Nuclei were stained in blue with Hoechst (1/100). Scale bar 10 μm. **b** Scheme of the BRET$^2$ assay using $\sigma_1$Rluc and GHS-R1a-GFP$^2$. **c** BRET occurs in HEK-293T cells transfected with a constant amount of cDNA (0.075 μg) for $\sigma_1$Rluc and increasing amounts of GHS-R1a-GFP$^2$ (from 0.5 to 3 μg cDNA) or $A_{2A}$R-GFP$^2$ (from 0.5 to 2.5 μg cDNA) as negative control. Values are the mean (in milliBRET units: mBU) ± S.E.M. from six to eight different experiments

Next, we investigated the GHS-R1a TM domains involved in the interaction with $\sigma_1$R. Remarkably, in HEK-293T cells co-expressing GHS-R1a-nYFP (0.75 μg cDNA) and $\sigma_1$R-cYFP (0.5 μg cDNA), fluorescence complementation (4,000 units, which confirms the formation of GHS-R1a-$\sigma_1$R complexes as shown in confocal images (Supplementary Fig. 1A)) was significantly reduced in the presence of TM1, TM2, or TM5 peptides; a marked tendency without statistical significance in the case of TM6 peptide was also found (Fig. 2e). This clearly indicates the existence of two different interacting interfaces between GHS-R1a and $\sigma_1$R, involving either TM 1/2 or TM 5/6 interfaces of GHS-R1a and the single TM helix of $\sigma_1$R. When similar experiments were performed with $\sigma_1$R-cYFP (0.5 μg cDNA) and GHS-R1b-nYFP (0.5 μg cDNA), the fluorescent signal (3,500 units) decreased in the presence of TM1 and TM2 but not TM5 or TM6 peptides (Fig. 2f); it should be noted again that GHS-R1b lacks TMs 6 and 7. All members of the GPCR family retain analogous tertiary structures at the seven-helical-bundle domain; thus, we hypothesized that TM 1/2 or TM 5/6 interfaces could be involved in the interaction between the GPCRs and $\sigma_1$R. In addition, GPCR homo/heteromerization must be taken into account to accommodate the $\sigma_1$ receptor in the trimeric structure elucidated from structural studies. To obtain data in a more physiological set-up, HEK-293T cells were transfected with cDNAs for GHS-R1a-nYFP and $\sigma_1$R-cYFP in the presence of non-fused GHS-R1b. As fluorescence complementation (5,000 fluorescence units) was reduced only by TM1 and TM2 (Fig. 2g); our interpretation was that the formation of the GHS-R1a-GHS-R1b heterotetramer via TM 4/5 and TM 5/6 interfaces (Fig. 2d) only permits $\sigma_1$R to interact with GHS-R1a via the free TM 1/2 interface. Proper interference action of TM-TAT peptides was tested by PLA (Supplementary Fig. 1B). In fact, TM1 and TM2 TAT peptides blocked the expression of GHS-R1a-$\sigma_1$R heteromers while treatment with the TM7 TAT did not affect the PLA signal.

Using structural details on TM interfaces of GPCR oligomers [22] and the crystal structure of human $\sigma_1$R [23], together with the results from BiFC experiments performed in the absence and presence of disrupting TM peptides, we constructed a computational molecular model (see "Methods") of the GHS-R1a homodimer in complex with $G_i$ and $\sigma_1$R (Fig. 2h). The model of the GHS-R1a homodimer contains two free TM 4/5 interfaces that would allow binding of two GHS-R1b protomers (Fig. 2d). The crystal structure of $\sigma_1$R, in which the protein arranges as a homotrimer, suggests that the homotrimer may represent the functional unit [23]. Accordingly, we constructed a computational model consisting of the GHS-R1 dimer, a $\sigma_1$R trimer, and a G protein that fits with the requirements of the biochemical data and takes into account all available structural constraints (Fig. 2g; see "Methods"). According to the experiments with GHS-R1a-derived peptides (see above), $\sigma_1$R can bind GHS-R1b through the TM1/2 interface and GHS-R1a through either the TM1/2 or the TM5/6 interfaces. Because GHS-R1a and GHS-R1b also employ the TM5/6 interface for

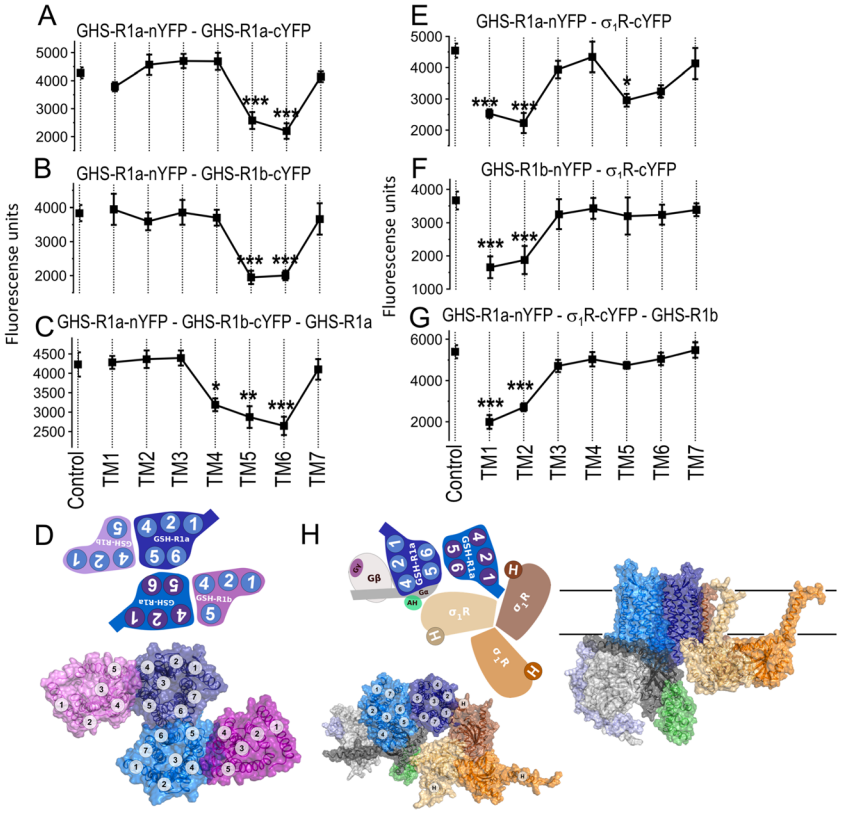


**Fig. 2** Effect of interfering peptides on the $\sigma_1$R-GHS-R1a interaction. **a**–**c**, **e**–**g** BiFC complementation experiments were performed in HEK-293T cells transfected with 0.75 μg cDNA for GHS-R1a-nYFP and 0.75 μg cDNA for GHS-R1a-cYFP (**a**), with 0.75 μg cDNA for GHS-R1a-nYFP and 0.75 μg cDNA for GHS-R1b-cYFP (**b**), with 0.75 μg cDNA for GHS-R1a-nYFP and 0.75 μg cDNA for GHS-R1b-cYFP in the presence of 1.5 μg cDNA for GHS-R1a-nYFP (**c**), with 0.75 μg cDNA for GHS-R1a-nYFP and 0.75 μg cDNA for $\sigma_1$R-cYFP (**e**), with 0.5 μg cDNA for GHS-R1b-nYFP and 0.5 μg cDNA for $\sigma_1$R-cYFP (**f**), or with 0.75 μg cDNA for GHS-R1a-nYFP and 0.75 μg cDNA for GHS-R1b-cYFP (**g**) in the presence of 1.5 μg cDNA of GHS-R1a not fused. Prior to fluorescence determination, cells were treated with each of the interfering peptides (TM1 to TM7, 4 μM) during 4 h. Values are the mean ± S.E.M. from eight to 10 different experiments. One-way ANOVA followed by Dunnett's *post hoc* test showed a significant effect of treatments versus control conditions. $*p < 0.05$, $**p < 0.01$, and $***p < 0.001$. **d** Structural model for the GHS-R1a-GHS-R1b heterotetramer (GHS-R1a protomers: blue, GHS-R1b protomers: purple) viewed from the extracellular side (scheme of the arrangement—top—and three-dimensional model (—bottom—).**h** (left) Structural model consisting of a GHS-R1a homodimer (GHS-R1a $G_\alpha$-bound: light blue, GHS-R1a $G_\alpha$-unbound: dark blue) in complex with a $\sigma_1$R homotrimer (in red, orange, and yellow) coupled to $G_i$ (Gα Ras-like domain: light gray, Gα alpha helical domain: green, Gβ: dark gray, and Gγ: purple) viewed from the extracellular side. **h** (right) Same model as in panel **h** (left) but viewed across the plane of the membrane. Proteins are displayed with a transparent surface and a cartoon. TM helices are indicated by circles (1–7 in GHS-R1a , 1-5 in GHSR1b and H in $\sigma_1$R)

homo-/heterodimerization, we assumed that at normal expression levels, TM1/2 is the most likely interface for the GHS-R1-$\sigma_1$R complex, as TM5/6 is occupied by the GHS-R1 homodimer/heterodimer. This model indicates that a single GPCR protomer of GHS-R1a cannot simultaneously bind $\sigma_1$R via the TM 1/2 interface and a G protein due to a steric clash between the βγ subunits of $G_i$ and the intracellular voluminous C-terminal domain of $\sigma_1$R, containing a rigid cupin-like β-barrel fold that forms the buried ligand-binding site and the βγ subunits of $G_i$ (Supplementary Fig. S1). Thus, the minimal functional unit requires a GHS-R1a homodimer in which one protomer binds the G protein, and the second protomer is responsible for the binding of the $\sigma_1$R TM helix (Fig. 2h). Interestingly, this model predicts that the cytoplasmic domain of one protomer of the $\sigma_1$R trimeric structure interacts with the α-subunit of $G_i$.

## Cocaine Increases Colocalization of $\sigma_1$R and GHS-R1a at the Cell Surface

As cocaine binds $\sigma_1$R [36], which establishes direct interactions with ghrelin receptors as shown above, we hypothesized that cocaine affects ghrelin-mediated signals. First, we investigated the effect of cocaine in GHS-R1a expression. Immunocytochemical assays were performed in cells expressing $\sigma_1$R and GHS-R1a after addition of cocaine (30 μM, 30 min). Figure 3a shows that plasma membrane expression of $\sigma_1$R increased when these cells were treated with a physiologically relevant dose of cocaine [37]. A similar increase was observed when cells were incubated with the $\sigma_1$R agonist PRE-084 (100 nM, 30 min). The expression of GHS-R1a was not modified upon treatment with cocaine or PRE-084 but, interestingly, colocalization of $\sigma_1$R and GHS-R1a at the cell

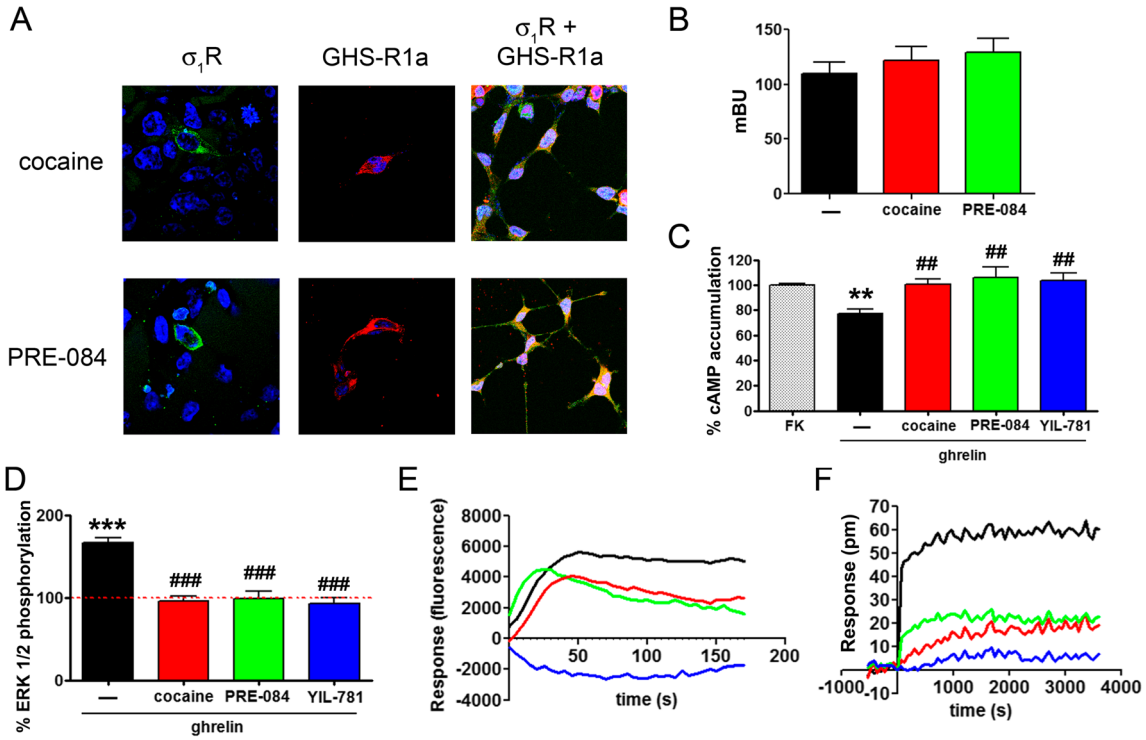


**Fig. 3** Effects of cocaine on ghrelin-mediated signaling. **a** HEK-293T cells transfected with 0.75 μg cDNA for $\sigma_1$R-YFP, 1.66 μg cDNA for GHS-R1a-Rluc, or both were treated with 30 μM cocaine or 100 nM PRE-084, then were monitored by the YFP fluorescence (green) or using a monoclonal anti-Rluc primary antibody and a cyanine-3-conjugated secondary antibody (red). Colocalization is shown in yellow. Nuclei were stained with Hoechst (blue). Scale bar 10 μm. **b** BRET in HEK-293T cells transfected with 0.075 μg cDNA for $\sigma_1$R-Rluc and 1.5 μg cDNA for GHS-R1a-GFP$^2$ and treated with 30 μM cocaine, 100 nM PRE-084, or vehicle for 30 min. Afterwards, the energy transfer signal was measured. Values are the mean ± S.E.M. of seven different experiments. One-way ANOVA followed by Dunnett's *post hoc* test did not show any significant effect of treatments versus control. **c–f** HEK-293T cells were transfected with 1.66 μg GHS-R1a cDNA and 0.25 μg GHS-R1b cDNA and treated with 30 μM of cocaine (red), 100 nM of the $\sigma_1$R agonist, PRE-084 (green), 2 μM of the GHS-R1a antagonist, YIL-781 (blue), or vehicle (black). Cells were then treated with ghrelin 100 nM (in (**c**), cells were treated with 0.5 μM forskolin (FK)). ERK1/2 phosphorylation (**d**) was analyzed using an AlphaScreen®SureFire® kit (Perkin Elmer). Fluorescence of the GCaMP6 sensor was used to monitor cytosolic calcium mobilization (**e**), and real-time label-free DMR tracings (**f**) representing the picometer shifts of reflected light wavelength were recorded in an EnSpire® Multimode Plate Reader (PerkinElmer, Waltham, MA, USA). Values are the mean ± S.E.M. from eight to 11 different experiments. One-way ANOVA followed by Dunnett's *post hoc* test showed a significant effect of treatments versus forskolin (cAMP assays, (**c**)) or control (pERK1/2 assays, (**d**)), and one-way ANOVA followed by Bonferroni's *post hoc* test showed a significant effect of treatments versus ghrelin, ##$p < 0.01$ and ###$p < 0.001$

surface increased. Thus, cocaine and the $\sigma_1$R-specific ligand PRE-084 are able to concomitantly affect co-expression of both receptors at the cell surface. Second, we evaluated the effect of cocaine and PRE-084 on the heteromerization of $\sigma_1$R and GHS-R1a. A tendency to increased energy transfer (without reaching statistical significance) was observed in the presence of cocaine (30 μM) or PRE-084 (100 nM) in HEK-293T cells transfected with 0.075 μg cDNA for $\sigma_1$R-Rluc and 1.5 μg cDNA for GHS-R1a-GFP$^2$ (Fig. 3b).

## Cocaine Inhibits GHS-R1a Signaling

We first evaluated the effect of cocaine and PRE-084 on GHS-R1a-mediated signaling by measuring cAMP levels. HEK-293T cells endogenously express $\sigma_1$R, but do not express ghrelin receptors [37]. Moreover, it is known that low concentrations of GHS-R1b expression significantly increase GHS-R1a signaling [21]. Thus, to analyze GHS-R1a signaling pathways in HEK-293T cells, we co-expressed GHS-R1a (1.66 μg cDNA) with low amounts of GHS-R1b (0.25 μg cDNA). Stimulation of these cells with ghrelin (100 nM) in the presence of forskolin (0.5 μM) significantly decreased cAMP levels (Fig. 3c). This agrees with the previously reported coupling of ghrelin receptors with $G_i$ (www.guidetopharmacology.org) [7]. The effect of ghrelin on forskolin-induced cAMP levels was completely blocked by pretreatment with the GHS-R1a selective antagonist YIL-781 (2 μM) (Fig. 3c). Interestingly, when cells were treated with cocaine (30 μM, 15 min) or the $\sigma_1$R agonist (PRE-084, 100 nM, 15 min) prior to ghrelin stimulation, the decrease in cAMP levels was prevented to the extent similar to the one occurring with the GHS-R1a selective antagonist YIL-781 (Fig. 3c). This suggests that cocaine behaves as agonist of $\sigma_1$R and inhibits GHS-R1a

signaling as efficiently as the GHS-R1a selective antagonist YIL-781 bound to the orthosteric binding site. Similar experiments were carried out in HEK-293T transfected with another class A GPCR. When the adenosine $A_1$R receptors were used instead of GHS-R1a, neither ghrelin, nor cocaine induced any effect (Supplementary Fig. 2A-B). Moreover, $A_1$ adenosine receptor expressing HEK-293T cells treated with a selective agonist (R-PIA, 100 nM) showed a significant decrease in cAMP and increase in MAPK phosphorylation that was abolished by the $A_1$ receptor antagonist (1 μM, DPCPX) but not by cocaine or PRE-084 (Supplementary Fig. 2C-D).

Measurement of ERK1/2 phosphorylation in HEK-293T cells transfected with GHS-R1a and GHS-R1b after stimulation with ghrelin shows an increase of 80% (Fig. 3d). Similarly to measurements of cAMP levels (Fig. 3c), the GHS-R1a selective antagonist YIL-781 and the $\sigma_1$R agonists cocaine and PRE-084 inhibited ghrelin effects (Fig. 3d). This indicates that cocaine and PRE-084 not only affect the $\alpha_i$-dependent pathway, but also the $\beta\gamma$-dependent signaling. Moreover, a characteristic trace of intracellular calcium transient levels was obtained in HEK-293T cells expressing GHS-R1a, GHS-R1b, and $\sigma_1$R after activation with ghrelin (Fig. 3e). The calcium signal was abrogated by the selective ghrelin receptor antagonist and was reduced by cocaine and by PRE-084. To further test the inhibitory effect of agonist binding to $\sigma_1$R in GHS-R1a, we performed dynamic mass redistribution (DMR) recordings that measure the changes in the wavelength of light passing through cell monolayer [38]. Once again, the magnitude of the signaling by ghrelin significantly decreased in the presence of YIL-781, cocaine and PRE-084 (Fig. 3f). We can, thus, conclude that the GHS-R1a selective antagonist YIL-781, cocaine, and PRE-084 inhibited ghrelin effects, as measured by cAMP levels, ERK1/2 phosphorylation, and DMR signal.

## Cocaine Inhibition of GHS-R1a Signaling Is Mediated by $\sigma_1$R

To check whether cocaine inhibition of ghrelin-induced signaling was due to its interaction with $\sigma_1$R, HEK-293T cells expressing GHS-R1a (1.66 μg cDNA) and GHS-R1b (0.25 μg cDNA) were transfected with a siRNA designed to knock down expression of $\sigma_1$R (3 μg siRNA). Cells incorporating siRNA responded to 100 nM of ghrelin in both forskolin-induced cAMP determination and ERK1/2 phosphorylation, with similar results to those in cells without siRNA (Fig. 4a, b). However, in the presence of siRNA, cocaine or PRE-084 had no effect on ghrelin-induced signals while pretreatment with YIL-781 blocked ghrelin-induced GHS-1a activation. Also, when HEK-293T cells expressing GHS-R1a were transfected with siRNA against $\sigma_1$R, ghrelin induced a characteristic signal on calcium mobilization or on DMR recordings. Similarly, these stimulations were not affected by cocaine or PRE-084 pretreatment, while they were completely blocked by the ghrelin antagonist YIL-781 (Fig. 4c, d). These results show that cocaine effects on GHS-R1a receptor are mediated by $\sigma_1$R.

## Disruption of the Heteromeric Complex Between $\sigma_1$R and GHS-R1a by the TM1 Interference Peptide Blocks the Effect of Cocaine on GHS-R1a Function

As proposed above from data using TAT-fused synthetic peptides, the single TM helix of $\sigma_1$R likely interacts with TMs 1 and 2 of GHS-R1a. Accordingly, we can hypothesize that addition of the TM1 interference peptide would abolish the effect of cocaine on GHS-R1a function. Thus, HEK-293T cells expressing GHS-R1a (1.66 μg cDNA) were treated during 4 h with 4 μM of TAT-TM1 (or TAT-TM7 as negative control). In agreement with our hypothesis, disruption of $\sigma_1$R-GHS-R1a heteromeric complex was achieved by TM1, but not by TM7 TAT peptides; in these experimental conditions in which TM1 peptide was present, only the GHS-R1a selective antagonist YIL-781 (1 μM) blocked ghrelin (100 nM) stimulation, whereas cocaine (30 μM) or PRE-084 (100 nM) did not display any effect on either cAMP levels (Fig. 4e, g) or DMR signals (Fig. 4f, h). These results demonstrate that disruption of the GHS-R1a-$\sigma_1$R interaction using TM1 alters the cocaine effect on ghrelin receptors, thus reinforcing the idea that cocaine modulates GHS-R1a receptor function via $\sigma_1$R.

Next, we attempted to provide insight into the mechanism by which cocaine binds to $\sigma_1$R and blocks GHS-R1a function. Our structural model predicts that a single protomer of GHS-R1a cannot simultaneously bind $\sigma_1$R (via the TM 1/2 interface) and $G_i$ (supplementary Fig. S1); accordingly, $\sigma_1$R may impede $G_i$ binding and, in consequence, GHS-R1a function. However, this does not seem reasonable due to the possible formation of a GHS-R1a homodimer in which one protomer binds $G_i$ and the second protomer binds $\sigma_1$R (Fig. 2h). Notably, this model positions the cytoplasmic domain of one protomer of the $\sigma_1$R trimeric structure near the α-helical domain (αAH) of the G protein α-subunit (Fig. 2h). It has been shown that the mechanism for receptor-catalyzed nucleotide exchange in G proteins involves a large-scale opening of αAH, from the *Ras* domain, allowing GDP to freely dissociate [39]. This opening of αAH is not feasible in the presence of the $\sigma_1$R trimeric structure bound to TMs 1 and 2 of GHS-R1a. Modification of the GHS-R1a-$\sigma_1$R interaction, by inserting the TAT-fused TM1 peptide, would increase the distance between cytoplasmic domain of $\sigma_1$R and αAH, facilitating Gi function, and these were the results found in our assays.

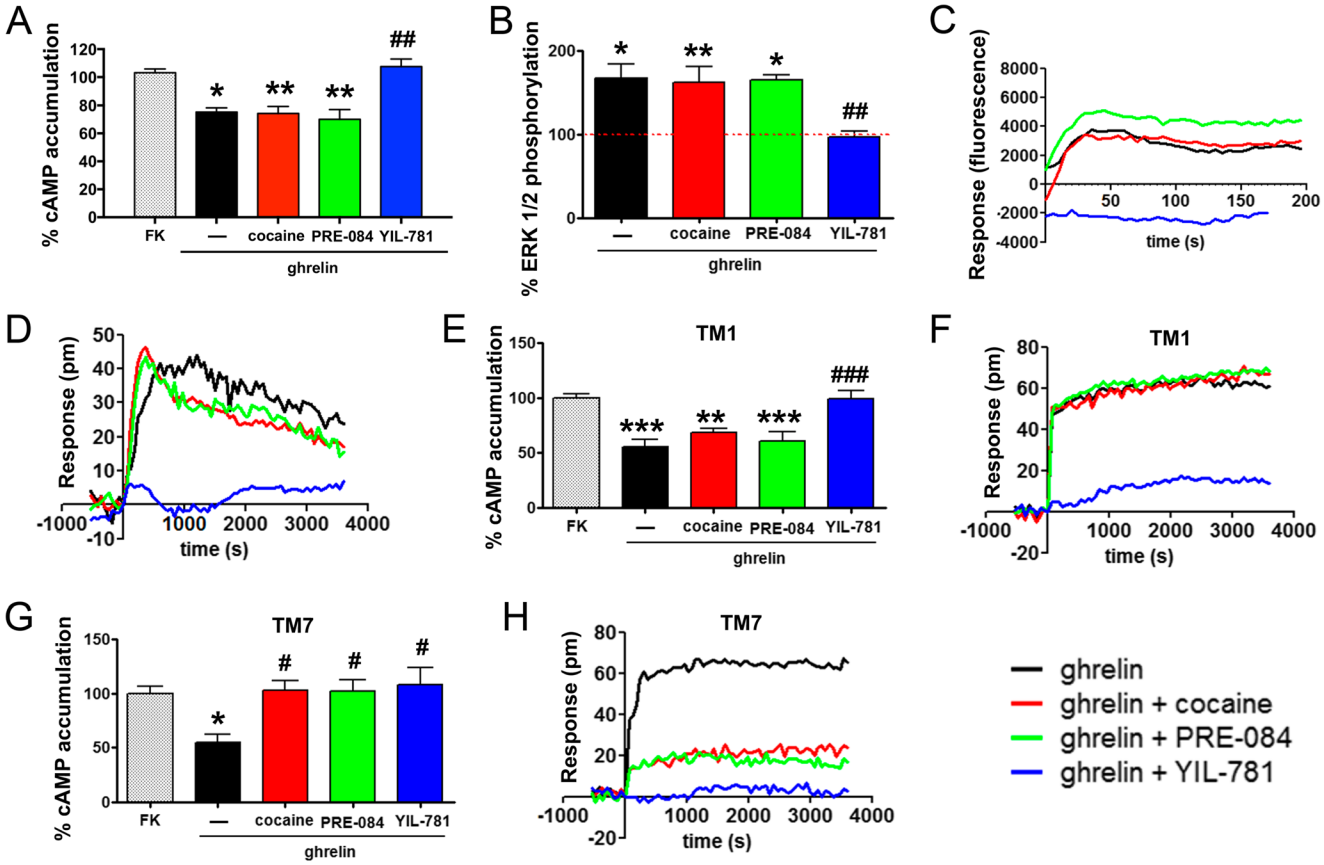


**Fig. 4** Effects of cocaine on GHs-R1a signaling are dependent on $\sigma_1$R expression. **a**–**d** HEK-293T cells were transfected with 1.66 μg GHS-R1a cDNA, 0.25 μg GHS-R1b cDNA, and 3 μg siRNA for $\sigma_1$R. These cells were treated with 30 μM of cocaine (red), 100 nM of the $\sigma_1$R agonist, PRE-084 (green), 2 μM of the GHS-R1a antagonist, YIL-781 (blue), or vehicle (black) followed by 100 nM of ghrelin stimulation (in (**a**), cells were treated with 0.5 μM forskolin). cAMP levels (**a**), pERK1/2 (**b**), calcium ion (**c**), and DMR (**d**) signals were recorded. Values are the mean ± S.E.M. from eight to 11 different experiments. One-way ANOVA followed by Dunnett's *post hoc* test showed a significant effect of treatments versus forskolin (cAMP assays, (**a**)) or control (pERK1/2 assays, (**b**)), $*p < 0.05$, $**p < 0.01$, and one-way ANOVA followed by Bonferroni's *post hoc* test showed a significant effect of treatments versus ghrelin, $\#\#p < 0.01$. **e**–**f** HEK-293T cells expressing GHS-R1a (0.5 μg cDNA) were treated for 4 h with TM1 (**e**, **f**) or TM7 (**g**, **h**) TAT-peptides. Cells were subsequently treated with 30 μM cocaine (red), 100 nM PRE-084 (green), 1 μM YIL-781 (blue), or vehicle (black). Cells were then treated with 100 nM ghrelin ((in (**e**) and (**g**), cells were treated with 0.5 μM forskolin). Traces representing DMR signal variation over time are represented in **f** and **h**. Values are the mean ± S.E.M. of six different experiments. One-way ANOVA followed by Dunnett's *post hoc* test showed a significant effect of treatments versus forskolin, $*p < 0.05$, $**p < 0.01$, and $***p < 0.001$, and one-way ANOVA followed by Bonferroni's *post hoc* test showed a significant effect of treatments versus ghrelin, $\#p < 0.05$ and $\#\#\#p < 0.001$

## Effect of Cocaine Treatment on a Cell Line and on Primary Cultures of Striatal Neurons

Most of the cocaine effects in the central nervous system (CNS) occur in the striatum [40, 41]. Consequently, we analyzed cocaine effects on GHS-R1a expressed in the SH-SY5Y neuroblastoma cell line. Cells were transfected with cDNAs for GHS-R1a (1.66 μg), GHS-R1b (0.25 μg), and $\sigma_1$R (0.75 μg). The results were similar to those obtained in HEK-293T cells, i.e., cocaine and PRE-084 specifically blocked ghrelin action on cAMP levels and ERK1/2 phosphorylation (Fig. 5a, b). Pretreatment with the ghrelin receptor antagonist, YIL-781, also blocked ghrelin effects in neuroblastoma cells. Then, we moved to primary cultures of striatal neurons to analyze in a more physiological environment the cocaine effects over GHS-R1a receptors. The in situ proximity ligation assay (PLA), which allows the identification of interactions between two proteins in close proximity (< 17 nm) [10, 42, 43] was used to identify GHS-R1a-$\sigma_1$R complexes, detected as punctate red marks surrounding Hoechst-stained nuclei (Fig. 5a). In striatal primary cultures, 43% of cells presented red dots with two dots/cell-containing dots. However, when these cells were treated with 30 μM cocaine for 30 min, the number of cells containing red dots and the ratio of dots/cell-containing dots increased significantly (54% of cells presented red dots with 3.2 dots/cell-containing dots). These results indicate that cocaine pretreatment increases GHS-R1a-$\sigma_1$R complex formation in striatal primary cultures (Fig. 5a, b).

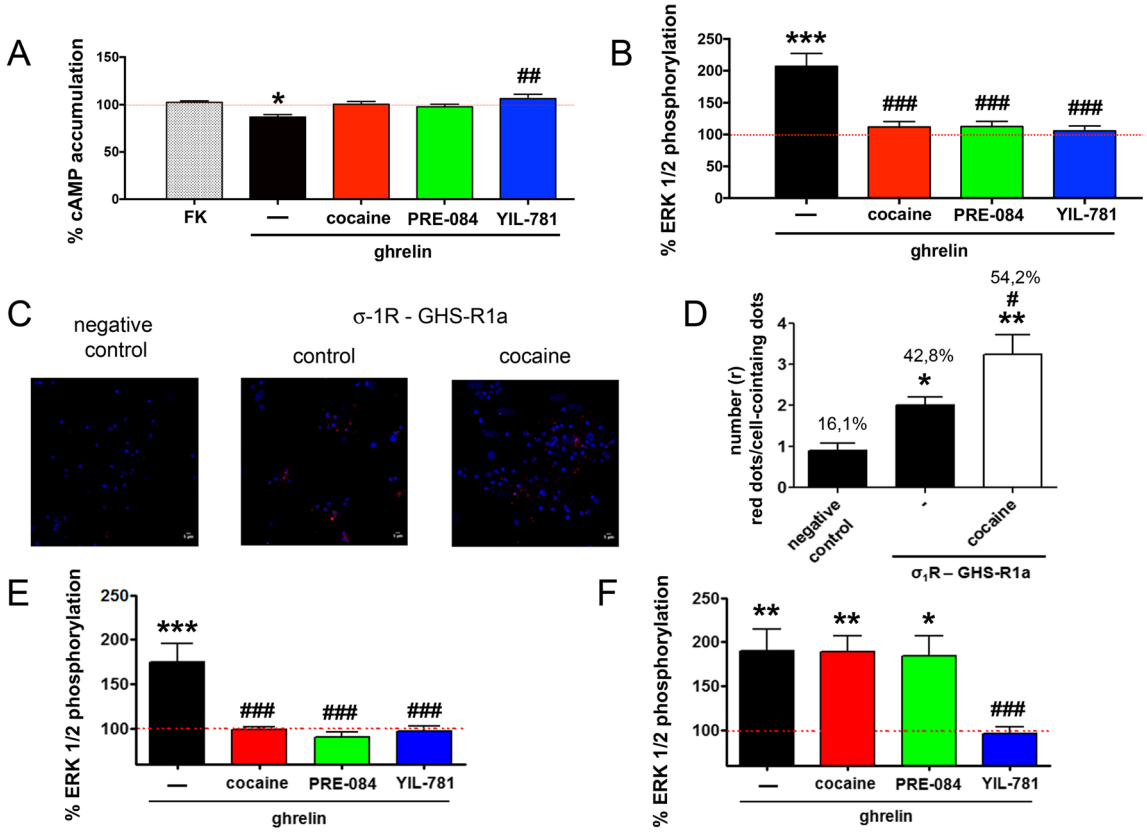


**Fig. 5** Cocaine treatment inhibited GHs-R1a signaling in primary cultures of striatal neurons. **a**, **b** SH-SY5Y cells were transfected with cDNAs for GHS-R1a (1.66 μg), GHS-R1b (0.25 μg), and $\sigma_1$R (0.75 μg). Assays were performed in transfected cells treated with 30 μM cocaine (red) cocaine, 100 nM of the $\sigma_1$R agonist, PRE-084 (green), 2 μM of the GHS-R1a antagonist, YIL-781 (blue), or vehicle (black) prior to 100 nM ghrelin addition. cAMP levels were determined after 15 min of 0.5 μM forskolin treatment (**a**). ERK1/2 phosphorylation (**b**) was determined using an AlphaScreen®SureFire® kit (Perkin Elmer). Values are ± S.E.M. from five to six different experiments. One-way ANOVA followed by Dunnett's *post hoc* test showed a significant effect of treatments versus forskolin (cAMP assay) or versus control (ERK phosphorylation assay), $*p < 0.05$, $**p < 0.01$, and $***p < 0.001$, and one-way ANOVA followed by Bonferroni's *post hoc* test showed a significant effect of treatments versus ghrelin, $\#\#p < 0.01$ and $\#\#\#p < 0.001$. In **c**, **d**, GHS-R1a-$\sigma_1$R heteroreceptor complexes were identified in striatal primary cultures treated with 30 μM cocaine, 100 nM PRE-084, or vehicle and detected by PLA (see "Methods") using a polyclonal anti-$\sigma_1$R primary antibody (1/100, Santa Cruz Biotechnology, Dallas, US) and a polyclonal anti-ghrelin primary antibody (1/100, AbCam, Cambridge, UK). Nuclei were labeled using Hoechst (1/100). **c** Representative confocal images showing GHS-R1a-$\sigma_1$R complexes as red dots surrounding Hoechst-stained nuclei. Scale bar, 5 μm. **d** Percentage of positive cells (containing one or more red dots in cells in five–six different fields), and number (r) of red dots/cell-containing dots in primary cultures of striatal neurons. One-way ANOVA followed by Dunnett's *post hoc* test showed a significant effect of treatments versus the negative control, $*p < 0.05$, $**p < 0.01$, and one-way ANOVA followed by Bonferroni's *post hoc* test showed a significant effect of treatments versus the untreated cells, $\#p < 0.05$. **e**, **f** Striatal primary cultures transfected (**f**) or not (**e**) with 3 μg siRNA for $\sigma_1$R were treated with 30 μM cocaine (red), 100 nM of the $\sigma_1$R agonist, PRE-084 (green), 2 μM of the GHS-R1a antagonist, YIL-781 (blue), or vehicle (black) prior to 100 nM ghrelin addition. ERK1/2 phosphorylation (**e**, **f**) was analyzed using an AlphaScreen®SureFire® kit (Perkin Elmer). Values are ± S.E.M. from six to eight different experiments. One-way ANOVA followed by Dunnett's *post hoc* test showed a significant effect of treatments versus control, $*p < 0.05$, $**p < 0.01$, and $***p < 0.001$, and one-way ANOVA followed by Bonferroni's *post hoc* test showed a significant effect of treatments versus ghrelin, $\#\#\#p < 0.001$

Cocaine effects on GHS-R1a signaling were further analyzed in primary cultures of striatal neurons, both in cAMP level determination and in ERK1/2 phosphorylation assays. Cocaine and PRE-084 counteracted the ghrelin-induced GHS-R1a signaling in a similar way as the GHS-R1a-specific antagonist YIL-781 (Fig. 5c, d). Such effect of cocaine was related to $\sigma_1$R modulation of GHS-R1a, as in striatal primary cultures treated with siRNA for $\sigma_1$R, neither cocaine nor PRE-084 achieved any significant effect (Fig. 5e, f).

## Effect of Cocaine Administration on GHS-R1a-$\sigma_1$R Heteromer Expression in Striatal Sections from Naïve and Cocaine-Treated Animals

Following i.p. administration of 15 mg/kg cocaine for 1 (acute) or 14 (chronic) days, rats were sacrificed, and 30 μm thick striatal sections were obtained from each group of animals and from vehicle-treated animals. The in situ proximity ligation assay (PLA) was used to identify GHS-R1a-$\sigma_1$R heteroreceptor complexes (Fig. 6a). When striatal sections of

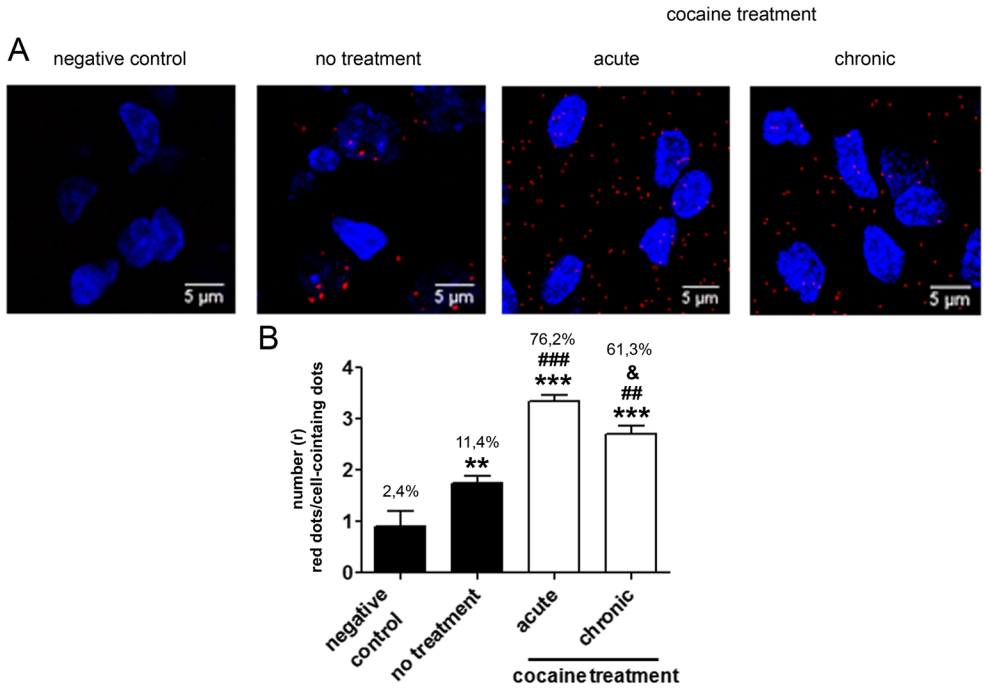


**Fig. 6** Acute and chronic cocaine treatment increase the GHS-R1a-$\sigma_1$R heteromer expression in the rat striatum. Male Sprague-Dawley rats were i.p. administrated with vehicle (control) or 15 mg/kg cocaine for 1 (acute) or 14 (chronic) days. To identify σ1-GHS-R1a complexes from each condition, rats were sacrificed and 30 µm thick striatal sections were obtained and treated with a polyclonal anti-$\sigma_1$R primary antibody (1/100, Santa Cruz Biotechnology, Dallas, US) and a polyclonal anti-ghrelin primary antibody (1/100, AbCam, Cambridge, UK) in the presence of Hoechst (1/100) and then treated with the PLA probes (see "Methods"). Representative PLA confocal images showing GHS-R1a-$\sigma_1$R complexes as red dots surrounding Hoechst-stained nuclei are shown for each condition (Fig. 6a). Scale bar, 5 µm. **b** Percentage of positive cells (containing one or more red dots; from cells in four–six different fields) and number (r) of red dots/cell-containing dots in rat striatal sections. One-way ANOVA followed by Dunnett's *post hoc* test showed a significant effect of treatments versus the negative control, $*p < 0.05$, $**p < 0.01$, one-way ANOVA followed by Bonferroni's *post hoc* test showed a significant effect of treatments versus the untreated cells, $\#\#\#p < 0.001$, and one-way ANOVA followed by Bonferroni's *post hoc* test showed a significant effect of chronic treatment versus acutely treated sections, $\&p < 0.05$

vehicle-treated animals were analyzed, it was observed that 11% of cells showed red dots with 1.6 dots/cell-containing dots (Fig. 6b), indicating that around 10% of striatal cells expressed GHS-R1a-$\sigma_1$R complexes. Interestingly, in the case of the chronic treatment, the number of cells containing dots strongly increased to 61%, and also, the number of dots/cell-containing dots (2.7) was significantly higher compared to control cells. Remarkably, the cocaine acute treatment leads to values that were even higher than in the chronic condition (76% of cells containing dots and 3.2 dots/cell-containing dots). These results indicate that cocaine treatment modulated GHS-R1a-$\sigma_1$R complex formation in striatal rat sections with a maximum increase in heteromer formation found in acute conditions (Fig. 6b).

## Discussion

The endogenous ligand of $\sigma_1$R remains unknown; however, synthetic agonists and antagonists are available. PRE-084 is a selective agonist due to its ability to dose-dependently dissociate $\sigma_1$R from a binding immunoglobulin protein/78 kDa glucose-regulated protein (BiP/GPR-78) [44]. Despite not being associated with a specific signaling machinery, $\sigma_1$R operates via translocation to the plasma membrane and via protein-protein-mediated modulation of cell responses upon agonist activation [11]. The mechanism involves calcium signaling and ion channel activation [45] and, in addition, the regulation of GPCR function [11]. For instance, it has been shown that $\sigma_1$R is involved in the negative control that glutamate N-methyl-D-aspartate acid receptors (NMDARs) exert on opioid antinociception [46]. Thus, $\sigma_1$R antagonists would enhance antinociception and reduce neuropathic pain induced by µ-opioid receptors. Another remarkable example is the control of $\sigma_1$R in the interaction between cannabinoid CB1 and NMDA receptors, whose functional unbalance constitutes a vulnerability factor for cannabis abuse, potentially precipitating schizophrenia [47]. Upon demonstrating that cocaine binds to $\sigma_1$R even at doses attained at recreational use, $\sigma_1$R is proposed to mediate locomotor activation [48, 49], seizures [18], drug sensitization [50], and reward actions [51, 52]. Reduction of $\sigma_1$R levels by injection of antisense nucleotides results in attenuating the convulsive effects of the drug [53], whereas the action of $\sigma_1$R agonists or antagonists exacerbates

or minimizes, respectively, cocaine effects [53–55]. Although activation of $\sigma_1$R by agonists is also involved in the appetitive properties of cocaine [52], the underlying mechanism remains unknown. In this manuscript, we reveal for the first time that $\sigma_1$Rs mediate the *hunger-suppressive* action of cocaine by interacting with orexigenic ghrelin receptors.

The nucleus accumbens, one of the structures that form the striatum, is part of the reward system. Activation of this system in response to food intake produces a pleasant sensation and other primordial needs for mammalian survival [56]. It should be noted that in these mesolimbic regions, GHS-R1a is co-expressed in neurons with cocaine-sensitive $\sigma_1$R. From both mechanistic and molecular point of views, this report highlights an interaction between $\sigma_1$R and GHS-R1a that is translated into a strong inhibition of ghrelin-induced GHS-R1a signaling, as measured by G protein-dependent (cAMP accumulation and calcium release assays) and partly/fully G protein-independent (MAPK phosphorylation and dynamic mass redistribution assays) signaling pathways. We have shown in transfected HEK-293T cells and in striatal primary cultures of neurons that pretreatment with the $\sigma_1$R agonists cocaine or PRE-084 inhibits ghrelin-mediated signaling in a similar manner as the GHS-R1a antagonist YIL-781. This effect is mediated by $\sigma_1$R, because, in $\sigma_1$R-siRNA-treated cells, cocaine or PRE-084 had no effect on ghrelin-induced signals while the ghrelin receptor antagonist, YIL-781, maintained its effect.

Kotagale and collaborators [57] have described the potent orexigenic effects of neuropeptide Y (NPY), which was described in autoradiographic studies [58] as a possible endogenous ligand for a subpopulation of sigma receptors, thus linking the stimulation of sigma receptors with hunger. It turned out that the action of NPY on sigma receptors could not be reproduced, i.e., no high affinity binding of NPY to brain sigma receptors can be measured [59]. Our results show that cocaine binding to $\sigma_1$R could counteract the feeling of hunger by a mechanism that excludes a direct competition between cocaine and NPY to interact with $\sigma_1$R. The proposed formation of the $\sigma_1$R-GHS-R1a interaction becomes even more important by the finding that heteromer expression is increased in both acute and chronic cocaine administration. However, the effect was more marked in acute conditions. In fact, striatal sections of Sprague-Dawley rats injected for 1 day with 15 mg/kg cocaine displayed threefold higher expression of $\sigma_1$R-GHS-R1a heteromers than the control animals.

The structure of $\sigma_1$R has traditionally considered to be formed by two TM helices. However, the recently released crystal structure of $\sigma_1$R has shown homotrimers whose protomers contain a single TM domain and a C-terminal domain having a buried ligand-binding site [27]. We have proposed, from data using TAT-fused synthetic peptides together with BiFC assays, that this single TM helix of one $\sigma_1$R molecule can be recognized by two different interacting interfaces of the 7TM bundle of GHS-R1a, either by interfaces formed by TMs 1 and 2 or TMs 5 and 6. Oligomerization of GPCRs via a particular interface likely guides the interacting interface in the $\sigma_1$R. The same TM helices may be involved in interactions of $\sigma_1$R with other GPCRs. In the particular case of $\sigma_1$R-GHS-R1a, due to the formation of the GHS-R1a-GHS-R1b heterotetramer via TM 4/5 and TM 5/6 interfaces, $\sigma_1$R can interact with GHS-R1a via the free TM 1/2 interface. We would like to speculate that, because $\sigma_1$R is a homotrimer, the two additional TM helices can bind two additional GHS-R1a-GHS-R1b heterotetramers, suggesting the possible ocurrence of higher order complexes formed by GHS-R1a and $\sigma_1$R, produced by successive combination of these units. These clusters may form specialized machineries of $\sigma_1$R-mediated signaling.

**Funding Information** This work was supported by grants from the Spanish Ministry of Innovation and Competitiveness (MINECO Ref. No. BFU2015-664405-R, SAF2015-74627-JIN and SAF2016-77830-R; they may include FEDER European Union funds).

## Compliance with Ethical Standards

**Conflict of Interest** The authors declare that they have no conflict of interests.

## References

1. Howick K, Griffin B, Cryan J, Schellekens H (2017) From belly to brain: targeting the ghrelin receptor in appetite and food intake regulation. Int J Mol Sci 18:273. https://doi.org/10.3390/ijms18020273
2. Cassidy RM, Tong Q (2017) Hunger and satiety gauge reward sensitivity. Front Endocrinol (Lausanne) 8:104. https://doi.org/10.3389/fendo.2017.00104
3. Conn PM, Bowers CY (1996) A new receptor for growth hormone-release peptide. Science 273:923–920
4. Geelissen SME, Beck IME, Darras VM, Kühn ER, van der Geyten S (2003) Distribution and regulation of chicken growth hormone secretagogue receptor isoforms. Gen Comp Endocrinol 134:167–174
5. Chan C-B, Cheng CH (2004) Identification and functional characterization of two alternatively spliced growth hormone secretagogue receptor transcripts from the pituitary of black seabream Acanthopagrus schlegelii. Mol Cell Endocrinol 214:81–95. https://doi.org/10.1016/j.mce.2003.11.020
6. Mary S, Fehrentz J-A, Damian M, Gaibelet G, Orcel H, Verdié P, Mouillac B, Martinez J et al (2013) Heterodimerization with its splice variant blocks the ghrelin receptor 1a in a non-signaling conformation: a study with a purified heterodimer assembled into lipid discs. J Biol Chem 288:24656–24665. https://doi.org/10.1074/jbc.M113.453423
7. Navarro G, Aguinaga D, Angelats E, Medrano M, Moreno E, Mallol J, Cortés A, Canela EI et al (2016) A significant role of the truncated ghrelin receptor GHS-R1b in ghrelin-induced signaling in neurons. J Biol Chem 291:13048–13062. https://doi.org/10.1074/jbc.M116.715144
8. Chow KBS, Sun J, Chu KM et al (2012) The truncated ghrelin receptor polypeptide (GHS-R1b) is localized in the endoplasmic

reticulum where it forms heterodimers with ghrelin receptors (GHS-R1a) to attenuate their cell surface expression. Mol Cell Endocrinol 348:247–254. https://doi.org/10.1016/j.mce.2011.08.034

9. Damian M, Mary S, Maingot M, M'Kadmi C, Gagne D, Leyris JP, Denoyelle S, Gaibelet G et al (2015) Ghrelin receptor conformational dynamics regulate the transition from a preassembled to an active receptor:Gq complex. Proc Natl Acad Sci 112:1601–1606. https://doi.org/10.1073/pnas.1414618112
10. Borroto-Escuela DO, Brito I, Romero-Fernandez W, di Palma M, Oflijan J, Skieterska K, Duchou J, van Craenenbroeck K et al (2014) The G protein-coupled receptor heterodimer network (GPCR-HetNet) and its hub components. Int J Mol Sci 15:8570–8590. https://doi.org/10.3390/ijms15058570
11. Su TP, Su TC, Nakamura Y, Tsai SY (2016) The Sigma-1 receptor as a pluripotent modulator in living systems. Trends Pharmacol Sci 37:262–278. https://doi.org/10.1016/j.tips.2016.01.003
12. Corbera J, Vaño D, Martínez D, Vela JM, Zamanillo D, Dordal A, Andreu F, Hernandez E et al (2006) A medicinal-chemistry-guided approach to selective and druglike sigma-1 ligands. ChemMedChem 1:140–154. https://doi.org/10.1002/cmdc.200500034
13. Mei J, Pasternak GW (2002) Sigma1 receptor modulation of opioid analgesia in the mouse. J Pharmacol Exp Ther 300:1070–1074
14. Sun H, Shi M, Zhang W, Zheng YM, Xu YZ, Shi JJ, Liu T, Gunosewoyo H et al (2016) Development of novel alkoxyisoxazoles as sigma-1 receptor antagonists with antinociceptive efficacy. J Med Chem 59:6329–6343. https://doi.org/10.1021/acs.jmedchem.6b00571
15. McCracken KA, Bowen WD, de Costa BR, Matsumoto RR (1999) Two novel sigma receptor ligands, BD1047 and LR172, attenuate cocaine-induced toxicity and locomotor activity. Eur J Pharmacol 370:225–232
16. Skuza G (1999) Effect of sigma ligands on the cocaine-induced convulsions in mice. Pol J Pharmacol 51:477–483
17. Lever JR, Fergason-Cantrell EA, Watkinson LD, Carmack TL, Lord SA, Xu R, Miller DK, Lever SZ (2016) Cocaine occupancy of sigma $_1$ receptors and dopamine transporters in mice. Synapse 70:98–111. https://doi.org/10.1002/syn.21877
18. Matsumoto RR, Hewett KL, Pouw B, Bowen WD, Husbands SM, Cao JJ, Hauck Newman A (2001) Rimcazole analogs attenuate the convulsive effects of cocaine: correlation with binding to sigma receptors rather than dopamine transporters. Neuropharmacology 41:878–886. https://doi.org/10.1016/S0028-3908(01)00116-2
19. Marcellino D, Navarro G, Sahlholm K, Nilsson J, Agnati LF, Canela EI, Lluís C, Århem P et al (2010) Cocaine produces D2R-mediated conformational changes in the adenosine A(2A)R-dopamine D2R heteromer. Biochem Biophys Res Commun 394:988–992. https://doi.org/10.1016/j.bbrc.2010.03.104
20. Navarro G, Moreno E, Bonaventura J, Brugarolas M, Farré D, Aguinaga D, Mallol J, Cortés A et al (2013) Cocaine inhibits dopamine D2 receptor signaling via sigma-1-D2 receptor heteromers. PLoS One 8:e61245. https://doi.org/10.1371/journal.pone.0061245
21. Navarro G, Quiroz C, Moreno-Delgado D, Sierakowiak A, McDowell K, Moreno E, Rea W, Cai NS et al (2015) Orexin-corticotropin-releasing factor receptor heteromers in the ventral tegmental area as targets for cocaine. J Neurosci 35:6639–6653. https://doi.org/10.1523/JNEUROSCI.4364-14.2015
22. Cordomí A, Navarro G, Aymerich MS, Franco R (2015) Structures for G-protein-coupled receptor tetramers in complex with G proteins. Trends Biochem Sci 40:548–551. https://doi.org/10.1016/j.tibs.2015.07.007
23. Schmidt HR, Zheng S, Gurpinar E, Koehl A, Manglik A, Kruse AC (2016) Crystal structure of the human σ1 receptor. Nature 532:527–530. https://doi.org/10.1038/nature17391
24. Hradsky J, Mikhaylova M, Karpova A, Kreutz MR, Zuschratter W. Super-resolution microscopy of the neuronal calcium-binding proteins Calneuron-1 and Caldendrin. Methods Mol Biol. 2013;963:147–69. https://doi.org/10.1007/978-1-62703-230-8_10
25. Chen T.-W, Wardill T.J, Sun Y, Pulver S.R, Renninger S.L, Baohan A, Schreiter E.R, Kerr R.A et al (2013), Ultrasensitive fluorescent proteins for imaging neuronal activity. Nature 499:295–300. https://doi.org/10.1038/nature12354
26. Liu J, Yu B, Orozco-Cabal L, Grigoriadis DE, Rivier J, Vale WW, Shinnick-Gallagher P, Gallagher JP (2005) Chronic cocaine administration switches corticotropin-releasing Factor2 receptor-mediated depression to facilitation of glutamatergic transmission in the lateral septum. J Neurosci 25:577–583. https://doi.org/10.1523/JNEUROSCI.4196-04.2005
27. Schmidt HR, Zheng S, Gurpinar E, Koehl A, Manglik A, Kruse AC (2016) Crystal structure of the human?1 receptor. Nature 532:527–530. https://doi.org/10.1038/nature17391
28. Egloff P, Hillenbrand M, Klenk C, Batyuk A, Heine P, Balada S, Schlinkmann KM, Scott DJ et al (2014) Structure of signaling-competent neurotensin receptor 1 obtained by directed evolution in Escherichia coli. Proc Natl Acad Sci 111:E655–E662. https://doi.org/10.1073/pnas.1317903111
29. Krumm BE, White JF, Shah P, Grisshammer R (2015) Structural prerequisites for G-protein activation by the neurotensin receptor. Nat Commun 6:7895. https://doi.org/10.1038/ncomms8895
30. Rasmussen SGF, DeVree BT, Zou Y et al (2011) Crystal structure of the [bgr]2 adrenergic receptor-Gs protein complex. Nature 477:549–555. https://doi.org/10.1038/nature10361
31. Tesmer JJ, Berman DM, Gilman AG, Sprang SR (1997) Structure of RGS4 bound to AlF4-activated G(i alpha1): stabilization of the transition state for GTP hydrolysis. Cell 89:251–261
32. Manglik A, Kruse AC, Kobilka TS, Thian FS, Mathiesen JM, Sunahara RK, Pardo L, Weis WI et al (2012) Crystal structure of the μ-opioid receptor bound to a morphinan antagonist. Nature 485:321–326. https://doi.org/10.1038/nature10954
33. van Zundert GCP, Rodrigues JPGLM, Trellet M, Schmitz C, Kastritis PL, Karaca E, Melquiond ASJ, van Dijk M et al (2016) The HADDOCK2.2 web server: user-friendly integrative modeling of biomolecular complexes. J Mol Biol 428:720–725. https://doi.org/10.1016/j.jmb.2015.09.014
34. Ng GYK, O'Dowd BF, Lee SP et al (1996) Dopamine D2 receptor dimers and receptor-blocking peptides. Biochem Biophys Res Commun 227:200–204. https://doi.org/10.1006/bbrc.1996.1489
35. Hebert TE, Moffett S, Morello JP, Loisel TP, Bichet DG, Barret C, Bouvier M (1996) A peptide derived from a beta2-adrenergic receptor transmembrane domain inhibits both receptor dimerization and activation. J Biol Chem 271:16384–16392
36. Maurice T, Romieu P (2004) Involvement of the sigma1 receptor in the appetitive effects of cocaine. Pharmacopsychiatry 37(Suppl 3):S198–S207. https://doi.org/10.1055/s-2004-832678
37. Navarro G, Moreno E, Aymerich M, Marcellino D, McCormick PJ, Mallol J, Cortes A, Casado V et al (2010) Direct involvement of sigma-1 receptors in the dopamine D1 receptor-mediated effects of cocaine. Proc Natl Acad Sci U S A 107:18676–18681. https://doi.org/10.1073/pnas.1008911107
38. Grundmann M, Kostenis E (2015) Holistic methods for the analysis of cNMP effects. In: Handb. Exp. Pharmacol. pp 339–357
39. Dror RO, Mildorf TJ, Hilger D, Manglik A, Borhani DW, Arlow DH, Philippsen A, Villanueva N et al (2015) SIGNAL TRANSDUCTION. Structural basis for nucleotide exchange in heterotrimeric G proteins. Science 348:1361–1365. https://doi.org/10.1126/science.aaa5264
40. Joffe ME, Grueter BA (2016) Cocaine experience enhances thalamo-accumbens N-methyl-D-aspartate receptor function. Biol Psychiatry 80:671–681. https://doi.org/10.1016/j.biopsych.2016.04.002

41. Borroto-Escuela DO, Narváez M, Wydra K, Pintsuk J, Pinton L, Jimenez-Beristain A, di Palma M, Jastrzębska J et al (2017) Cocaine self-administration specifically increases A2AR-D2R and D2R-sigma1R heteroreceptor complexes in the rat nucleus accumbens shell. Relevance for cocaine use disorder. Pharmacol Biochem Behav 155:24–31. https://doi.org/10.1016/j.pbb.2017.03.003
42. Trifilieff P, Rives M-L, Urizar E, Piskorowski R, Vishwasrao H, Castrillon J, Schmauss C, Slättman M et al (2011) Detection of antigen interactions ex vivo by proximity ligation assay: endogenous dopamine D2-adenosine A2A receptor complexes in the striatum. Biotechniques 51:111–118. https://doi.org/10.2144/000113719
43. Fuxe K, Borroto-Escuela DO, Ciruela F, Guidolin D, Agnati LF (2014) Receptor-receptor interactions in heteroreceptor complexes: a new principle in biology. Focus on their role in learning and memory. Neurosci Discov 2:6
44. Hayashi T, Su T-P (2007) Sigma-1 receptor chaperones at the ER-mitochondrion interface regulate Ca(2+) signaling and cell survival. Cell 131:596–610. https://doi.org/10.1016/j.cell.2007.08.036
45. Wu Z, Bowen WD (2008) Role of sigma-1 receptor C-terminal segment in inositol 1,4,5-trisphosphate receptor activation: constitutive enhancement of calcium signaling in MCF-7 tumor cells. J Biol Chem 283:28198–28215. https://doi.org/10.1074/jbc.M802099200
46. Rodríguez-Muñoz M, Sánchez-Blázquez P, Herrero-Labrador R, Martínez-Murillo R, Merlos M, Vela JM, Garzón J. The σ1 receptor engages the redox-regulated HINT1 protein to bring opioid analgesia under NMDA receptor negative control. Antioxid Redox Signal. 2015 Apr 1;22(10):799–818. https://doi.org/10.1089/ars.2014.5993
47. Sánchez-Blázquez P, Rodríguez-Muñoz M, Herrero-Labrador R, Burgueño J, Zamanillo D, Garzón J (2014) The calcium-sensitive Sigma-1 receptor prevents cannabinoids from provoking glutamate NMDA receptor hypofunction: implications in antinociception and psychotic diseases. Int J Neuropsychopharmacol 17:1–13. https://doi.org/10.1017/S1461145714000029
48. Menkel M, Terry P, Pontecorvo M, Katz JL, Witkin JM (1991) Selective sigma ligands block stimulant effects of cocaine. Eur J Pharmacol 201:251–252
49. Barr JL, Deliu E, Brailoiu GC, Zhao P, Yan G, Abood ME, Unterwald EM, Brailoiu E (2015) Mechanisms of activation of nucleus accumbens neurons by cocaine via sigma-1 receptor-inositol 1,4,5-trisphosphate-transient receptor potential canonical channel pathways. Cell Calcium 58:196–207. https://doi.org/10.1016/j.ceca.2015.05.001
50. Ujike H, Kuroda S, Otsuki S (1996) Sigma receptor antagonists block the development of sensitization to cocaine. Eur J Pharmacol 296:123–128. https://doi.org/10.1016/0014-2999(95)00693-1
51. Romieu P, Martin-Fardon R, Maurice T (2000) Involvement of the sigma1 receptor in the cocaine-induced conditioned place preference. Neuroreport 11:2885–2888
52. Romieu P, Phan VL, Martin-Fardon R, Maurice T (2002) Involvement of the sigma(1) receptor in cocaine-induced conditioned place preference: possible dependence on dopamine uptake blockade. Neuropsychopharmacology 26:444–455. https://doi.org/10.1016/S0893-133X(01)00391-8
53. Matsumoto RR, McCracken KA, Pouw B et al (2002) Involvement of sigma receptors in the behavioral effects of cocaine: evidence from novel ligands and antisense oligodeoxynucleotides. Neuropharmacology 42:1043–1055
54. Matsumoto RR, Liu Y, Lerner M, Howard EW, Brackett DJ (2003) Sigma receptors: potential medications development target for anti-cocaine agents. Eur J Pharmacol 469:1–12
55. Matsumoto RR, Gilmore DL, Pouw B, Bowen WD, Williams W, Kausar A, Coop A (2004) Novel analogs of the σ receptor ligand BD1008 attenuate cocaine-induced toxicity in mice. Eur J Pharmacol 492:21–26. https://doi.org/10.1016/j.ejphar.2004.03.037
56. Kim HF, Hikosaka O (2015) Parallel basal ganglia circuits for voluntary and automatic behaviour to reach rewards. Brain 138:1776–1800. https://doi.org/10.1093/brain/awv134
57. Kotagale NR, Upadhya M, Hadole PN, Kokare DM, Taksande BG (2014) Involvement of hypothalamic neuropeptide Y in pentazocine induced suppression of food intake in rats. Neuropeptides 48:133–141. https://doi.org/10.1016/j.npep.2014.02.003
58. Roman FJ, Pascaud X, Duffy O, Vauche D, Martin B, Junien JL (1989) Neuropeptide Y and peptide YY interact with rat brain sigma and PCP binding sites. Eur J Pharmacol 174:301–302
59. Tam SW, Mitchell KN (1991) Neuropeptide Y and peptide YY do not bind to brain sigma and phencyclidine binding sites. Eur J Pharmacol 193:121–122